NOTICE CONCERNING COPYRIGHT RESTRICTIONS

Including Chemical Transport and Reaction In Numerical Geothermal Reservoir Models

Stephen P. White
Industrial Research Limited, P.O. Box 31-310,
Lower Hutt, New Zealand

SUMMARY

This paper presents two examples of large scale numerical models of geothermal reservoirs which include the transport of reacting chemicals. In the first example we consider the steady state chemical concentrations in a relatively hot, high gas-content, geothermal field. The chemical species included in the model are the gases CO_2 and H_2S, together with the main aqueous species associated with these gases. The second example considers permeability changes associated with the dissolution and deposition of silica as a convection cell is set up about a deep magma body

Introduction

Heat and mass transport and the interactions of fluid with the earth's crust are of interest for many reasons. The processes that may take place are diverse and include mineral dissolution and precipitation, redox reactions, gas-liquid interactions and biochemical reactions, to name but a few. Recently a number of researchers (e.g. Lichtner (1992), Steffel and Lasaga (1995) Bear and Nitao (1995) Friedly (1989), Friedly and Rubin (1992) White (1995)) have looked to combine hydrology and geochemistry to provide tools to study these processes.

White (1995) describes a method to treat the transport and reaction of chemicals in a geothermal setting. Chemical species concentrations often provide considerable insight into processes taking place within a geothermal reservoir. They may also be much more sensitive indicators of processes such as boiling and dilution taking place within the reservoir, than pressure and temperature measurements. Including chemical species concentrations in a numerical reservoir model and adjusting reservoir parameters to match measured physical (pressure, temperature etc.) and chemical data, has the potential to improve both the predictive capabilities of the model and to offer further insight into the processes taking place in the reservoir.

Kissling *et al.* (1996) included the chemistry associated with carbon dioxide in the Wairakei geothermal field. While this work was successful, it did expose several shortcomings in the software used to implement the method of White (1995) when applied to a large three-dimensional reservoir model. Several of these shortcomings were addressed in White and Kissling (1996), which introduced an improved algorithm to determine when phase changes take place in a reservoir containing dissolved gases and other aqueous species.

In this paper we firstly consider modelling the steady state of a gas-rich geothermal field. The example chosen is loosely based on the Rotokawa field located in the Taupo Volcanic Zone (TVZ) of New Zealand. The second example considers the evolution of a geothermal field and considers a kinetic reaction, the dissolution and deposition of silica. We include the effect of dissolution and deposition on rock permeability and porosity and calculate how these rock properties evolve with the field. We consider only the effect of silica dissolution/deposition, and ignore the role of thermal stresses and plastic or elastic
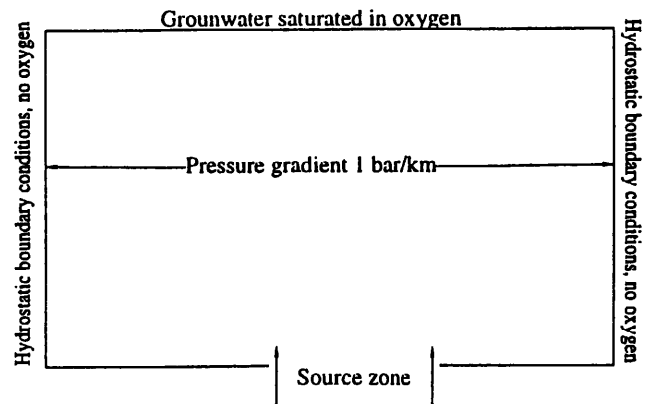
Figure 1. Cross section of field represented by model.

Table 1. Flow rates (m²) into source area, eq means flow rate is calculated from equilibrium equations.

Constituent	Flow rate (m²)
H^+	eq
OH^-	eq
CO_2	7.8×10^{-6} kg/s
HCO_3^-	eq
H_4SiO_4	eq
$H_3SiO_4^-$	eq
Cl^-	1.6×10^{-7} kg/s
HS^-	eq
O_2	0.0 kg/s
SO_4^-	0.0kg/s
H_2S	7.8×10^{-7} kg/s
CO_2-gas	0.0kg/s
H_2S-gas	0.0kg/s
water	1.6×10^{-5} kg/s
heat	23 J/s

deformation of the rock in creating and destroying permeability.

Model of a Gas-Rich Field

The numerical model described here is based on the Rotakawa geothermal field. It is intended to illustrate the concepts of chemical modelling rather than being a definitive model of the field.

We have used a modified version of the TOUGH2 (Pruess 1991) computer program that allows the inclusion of reacting chemicals as part of the model (White, 1995). This means that along with calculating pressure and temperature, we may also calculate concentrations of a number of chemical species. In some cases these species may be more sensitive indicators of processes occuring in the reservoir than temperature and pressure. We have included most of the reactions associated with the dissolution and transport of CO_2 and H_2S together with those associated with the main pH buffer (H_4SiO_4) believed to operate at Rotokawa. This gives a total of 11 aqueous species and two gases. We have not included any water-rock interactions such as mica and K-feldspar as these are considered to be too slow to affect changes induced by boiling. The reactions associated with the $CO_3^=$ ion have been neglected, as concentrations of this ion will be very small in fluids having a pH range of those found at Rotokawa. Chloride is included partly because it acts as a non-reacting species, and partly because Na^+ and Cl^- affect the activities of the other ions in solution.

We model the field in two dimensions, representing a vertical slice through the field. The area covered by the model is from near the ground surface to a depth of 3.5 kilometers with a length of ten kilometers. The grid used to model the reservoir contains 300 equal sized elements, constructed by dividing the

field into ten layers each of 350 meters thickness, and dividing each of these layers into 30 elements. Figure 1 is a schematic of the area modelled. The area labelled source region represents a region over which fluid containing a number of chemical species flows into the system. The flow rates of the various constituents of this fluid are give in Table 1. The left and right hand boundaries of the model are held at constant temperature and pressure, with the temperature increasing with depth at 30° C p/km, and the pressures are hydrostatic and consistent with this temperature gradient. Chemical concentrations at the side boundaries are assumed to be zero. The ground surface slopes downward from left to right and this gives rise to a pressure gradient across the field of about 1 bar / kilometer. The bottom of the model, other than the source zone, is treated as a no-flow boundary. The top of the model is water at 1 bar 20° C and saturated with oxygen. All other chemical concentrations are taken to be zero on this boundary.

The reactions considered are

$$H^+ + OH^- \Leftrightarrow H_2O$$

$$H_2O + CO_2 \Leftrightarrow HCO_3^- + H^+$$

$$H_4SiO_4 \Leftrightarrow H_3SiO_4^- + H^+$$

$$HS^- + 2O_2 \Leftrightarrow SO_4^= + H^+$$

$$CO_2\ (aq) \Leftrightarrow CO_2\ (gas)$$

$$H_2S\ (gas) \Leftrightarrow HS^- + H+$$
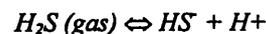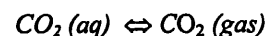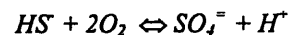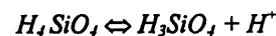
We assume equilibrium between chemical species and have taken temperature dependent equilibrium coefficients of the form

$$\text{Log}\ (K(T)) = \sum_{i=0}^{4} b_i T^i$$

The coefficients b_i have been taken from the SOLTHERM database (Reed and Spycher 1992).

Initially the reservoir is assumed to be cool with all chemical concentrations at zero. We then allow the model to evolve in time until changes in conditions over the field are small.

Modelling Results

Initially the system is taken to be at hydrostatic pressure with temperature increasing with depth at a rate of 30° per kilometer. The model is run until an approximate steady state is reached. The temperatures, pH and chemical species concentrations are shown in Figures 2-7. At steady state the reservoir has a two-phase zone over about a third of its length and above about one kilometer below the surface reaching to the surface. Waters in this two-phase zone are approximately neutral pH and with higher bicarbonate ion concentrations than the rest of the reservoir. In the downflow zone located at the left of the model we find high sulphate, low pH waters near the surface. These waters result from the oxidation of the H_2S in the upflow zone to form sulphuric acid by the oxygen saturated groundwa-
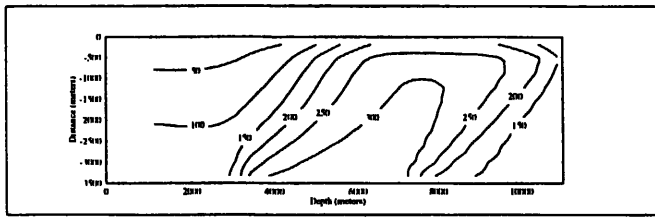
Figure 2. Steady state temperature contours.
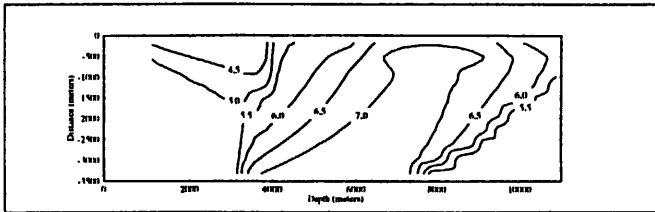
Figure 3. Reservoir pH at steady state.
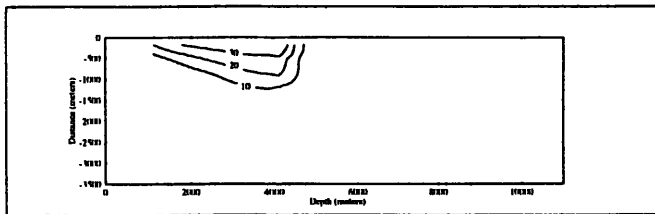
Figure 4. SO_4^- ×10^6 concentration at steady state (M/l).
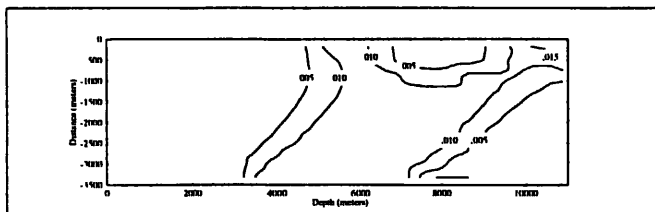
Figure 5. HCO_3^- ion concentration at steady state.
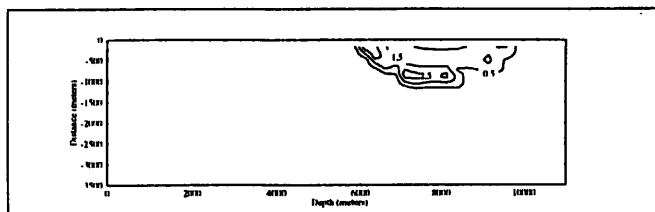
Figure 6. Partial pressure of CO_2 (bars) at steady state.
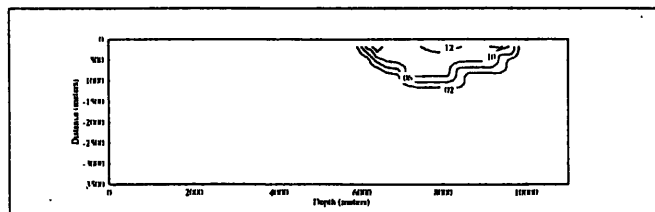
Figure 7. Partial pressure of H_2S (bars) at steady state

ter as it is drawn into the reservoir. The extent of the two-phase zone is shown in Figures 6 and 7 which are contours of the partial pressures of CO_2 and H_2S gases in the two-phase zone.

Evolution of a Geothermal Field

In this second example we consider the evolution of a geothermal field and include the transport, dissolution and precipitation of silica as part of the model. The model of the field is based on one of several investigated by Kissling (1997).

Silica Chemistry

There is a large dataset available on the solubility of quartz whose temperature and pressure range includes the region we are interested in modelling. In the near-neutral range, the dissolution reaction is pH independent and is usually written as

$$SiO_2(qtz) + 2H_2O = H_4SiO_4(aq) \qquad 1$$
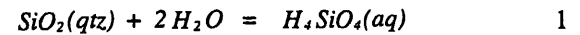
and the equilibrium constant is

$$K = \frac{a_{H_4SiO_4}}{a_{SiO_2}\, a^2_{H_2O}} \qquad 2$$

Providing the activity of water is one this simplifies to

$$K = a_{H_4SiO_4} \qquad 3$$

The only significant silicon species in solution is the neutral monomer, H_4SiO_4 (or $Si(OH)_4$). At supercritical temperatures and pressures there is still controversy about the hydration states of silica and Xie and Walther (1993a) prefer to write SiO for the neutral species. The thermodynamic properties of SiO and $Si(OH)_4$ are identical given the usual (normally most convenient) hypothetical standard state of unit molality where each of the species has the properties at infinite dilution at the temperature and pressure of interest.

Above about 200°C silica concentrations of hydrothermal fluids are controlled by the solubility of quartz so it is reasonable to assume that quartz solubility also accounts for large amounts of dissolved silica in sub and supercritical solutions.

The solubility of quartz in water has been measured over a wide range of conditions. Recently Manning (1994) published new results for quartz solubility between 500-900°C and 5-20 kb. He compared his results with the many previous published studies and presented an equation accurately reproducing measured quartz solubilities in water from 25°C and 1 bar to the conditions in his experiments. Data at temperatures less than 200°C and pressure up to 5 kb, were taken from Fournier and Potter (1982b). At the higher temperatures and pressures Manning's experimental results are slightly higher than predicted by Fournier and Potter (1982b). Their correlation was heavily weighted with data from a study which was shown by Manning (1994) to be subject to experimental problems. Thus at sub and supercritical temperatures the equation derived by Manning (1994) is preferred. His equation takes a form, depending only on temperature and the density of pure water (p).

$$\log K = A + \frac{B}{T} + \frac{C}{T^2} + \frac{D}{T^3} + \left[E + \frac{F}{T} + \frac{G}{T^2} \right] \log \rho_{H_2O} \quad 4$$

where the coefficients A-G are given in Table 2.

Table 2. Coefficients for Manning's equation, Equation (5).

A	B	C	D	E	F	G
4..26 20	-576 4.2	1.7513 x 10^6	-2.2869 x 10^8	2.84 54	-100 6.9	3.5689 x10^5

The solubility of quartz increases monotonically with pressure and temperature except for a region in the vicinity of the critical point, roughly between 200 and 1000 bar and 375 and 550°C, where the solubility decreases with temperature at constant pressure. This is the region of retrograde solubility where quartz may dissolve on cooling. In contrast log$K$ varies linearly with log (ρ_{H2O}) along isotherms.

Whether this phenomenon has wide significance for the evolution of hydrothermal systems is still being debated (Eugster, 1981). Fournier (1983a, 1985) has postulated that the precipitation of quartz in deep parts of a hydrothermal system may decrease permeability to such an extent that little convecting meteoric water can attain temperatures much greater than the quartz solubility maximum. The temperature at which deformation changes from frictional (brittle fracture) to quasi-plastic flow ranges from about 300 to 450°C. This overlaps the 375 to 550°C temperature range in which self sealing by the precipitation of quartz is likely to occur. Fournier concluded that the time interval over which meteoric water at hydrostatic pressure may interact directly with a shallow intruded body of magma may be limited to the early stages of development of the hydrothermal system, or episodically thereafter with creation of new fractures by tectonic activity or thermal or hydraulic cracking. Adding NaCl shifts the position of the retrograde field but does not change any of Fournier's conclusions.

Rates of Quartz Precipitation and Dissolution

There have been numerous investigations of quartz kinetics in pure water. Over the temperature range 150-300°C, Rimstidt and Barnes (1980) derived an E_a of 49.8 and 67.4-76.6 kJ/mol for quartz precipitation and dissolution in pure water respectively. Similarly Bird et al. (1986) found the $_a$ for precipitation to be 51-55 kJ/mol in the temperature range 121-255°C. The E_a for quartz dissolution derived in many other studies under different conditions ranged between 36 and 96 kJ/mol (Dove and Rimstidt, 1994). Recently Tester et al. (1994) correlated quartz dissolution kinetics in pure water using 5 different experimental apparatuses and 10 previous investigations, covering the temperature range 25 to 625°C. The E_a for dissolution was found to be 89±5 kJ/mol. Although this is higher than previously reported values, they had no reason to believe that there were errors in the dataset which may have resulted in an errone-

ously higher derived value. The empirical rate equation used was

$$r = k_f \frac{A_s}{M_s} \left(1 - \frac{m}{m_{sat}} \right) \quad 5$$

where r is the net rate (mol/kg-s), A_s is the active surface area (m^2), M_s is the mass of water (kg), k_f is the forward (dissolution) rate constant (mol/m^2-s) and m and m_{sat} are the molal and molal saturated concentrations of H_4SiO_4. The model is essentially the same as used by Rimstidt and Barnes (1980), Equation 21, except the rate law is based on concentrations rather than activities. The reverse rate constant can be predicted from the forward rate constant using

$$k_r = \frac{k_f}{m_{sat}} \quad 6$$

Dove (1994) derived a empirical rate equation which quantified the quartz reaction kinetics between 25 and 300°C, accounting for the combined the effects of pH (2 to 12) and the rate enhancing effects of alkali (0 to 0.3 molal). The equation is based on a surface complexation model of quartz.

$$r_{Dove} = exp^{-10.7} \, T exp \left(\frac{-66}{10^{-3}RT} \right) (\Theta_{>SiOH})^f$$

$$+ exp^{4.7} \, T exp \left(\frac{-82.7}{10^{-3}RT} \right) (\Theta_{>SiO_{ia}})^{f.1} \quad 7$$

where r $_{Dove}$ is the dissolution rate (mol/m^2-s), Θ_{SiOH} is the fraction of total surface sites occupied by hydrogen ion as θ>SiOH, $\Theta_{>SiO-tot}$ is the sum of all the fractions of total sites existing as deprotonated >SiO$^-$ and as a complex with sodium ion interaction.

The model predicts dissolution rates in variable solution compositions and temperatures and extends to give dissolution rates comparable to estimates at 385°C to 430°C by Murphy and Helegeson (1989) (Dove, 1984).

Dove's results are derived from dissolution experiments conducted so that the fluid remained very undersaturated with respect to silica. For the work described in this paper we have assumed a rate law based on Equation (7) of the form.

$$r = r_{Dove}(1 - \frac{Q}{K})$$

where r is the reaction rate (mole/m^2-s) K is the equilibrium constant, Q the ion activity quotient, r_{Dove} is the reaction rate constant given in equation (7).

The Numerical Model

Kissling (1997) and others have argued that a single magmatic intrusion provides insufficient heat to drive a geothermal field of the type typical of the Taupo Volcanic Zone of New
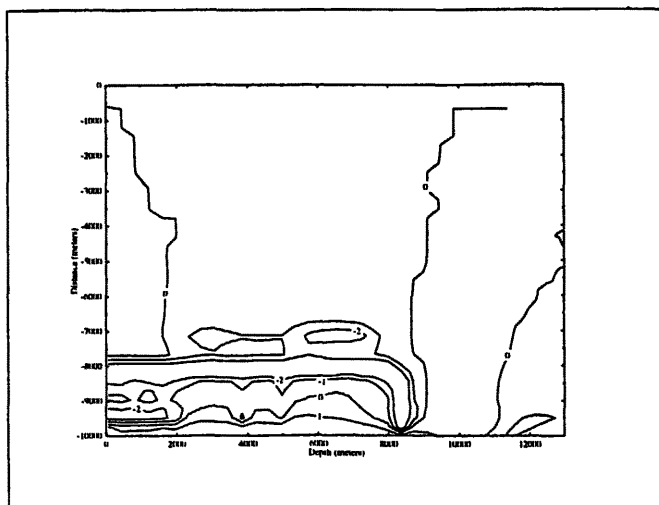
Figure 8. Log of permeability reduction factor at 100,000 years.
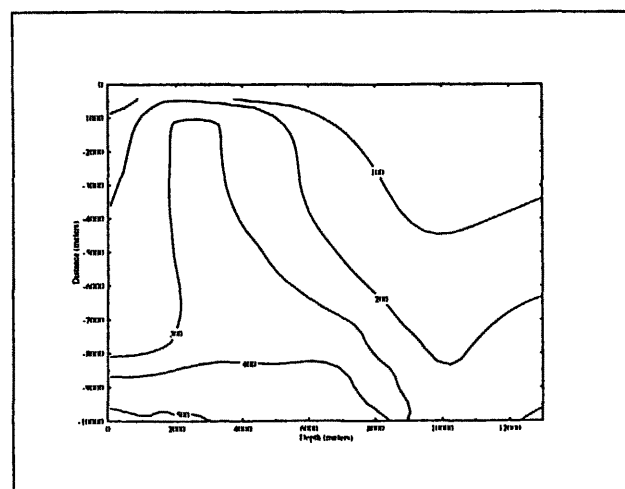
Figure 9. Temperature at 100,000 years.

Zealand. Kissling estimates that several hundred intrusions distributed spatially and in time are required to provide the energy dissipated by a geothermal field over it's lifetime. It is suggested that these intrusions can be represented by a single source with a constant output of heat and fluid. This source is much more extensive than a single magmatic intrusion. Kissling investigated the effect of varying the area of this source while keeping the total heat and mass output constant.

In this work we choose a source area of 26.4 square kilometers and model the source as an area of constant temperature (550 °C) at a depth of 10 kilometers together with an inflow of 600 °C fluid at a rate of 10kg/sec over this area. This mass flow rate is chosen to give approximately 5% magmatic water in the reservoir near the surface, which a typical magmatic water fraction for a western TVZ geothermal field. This source results in a total heatflow of about 260 MW, 200 MW by conduction and 60 MW from the magmatic fluid. We assume this magmatic fluid is saturated in silica.

For this preliminary work we have adopted a very simple permeability structure, a constant permeability of 0.01 milli-Darcys throughout the reservoir. Porosity ranges from .01 in the deepest layer to .2 in the shallow layers. A key rock property governing silica precipitation is the surface area of rock available for interaction with the reservoir fluid. We have taken this to be 2.5×10^5 m^2/m^3 throughout the reservoir. Clearly permeability, porosity and surface area are related and should all be varied throughout the reservoir, however doing this would not alter the general behaviour found in this work.

Results

The system is initially assumed to be at hydrostatic pressure, with a pressure of ten bars at the top of the model and a linear temperature profile from 20° C at the top of the model to 300° C at the base. This system is allowed to evolve under the influence of the boundary conditions and mass inflow. The change
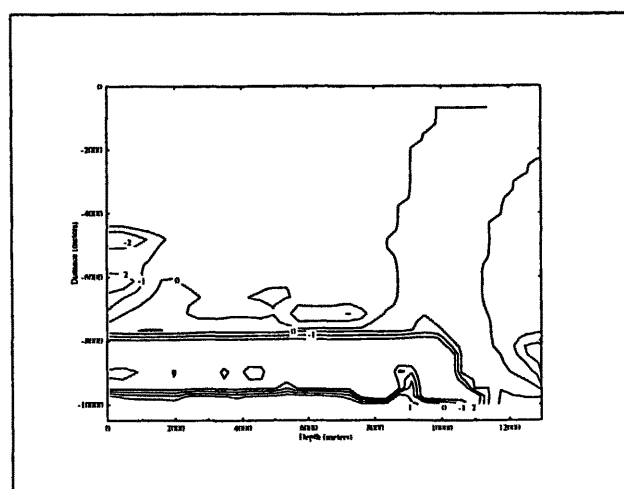
Figure 10. Log of permeability reduction factor at 600,000 years.
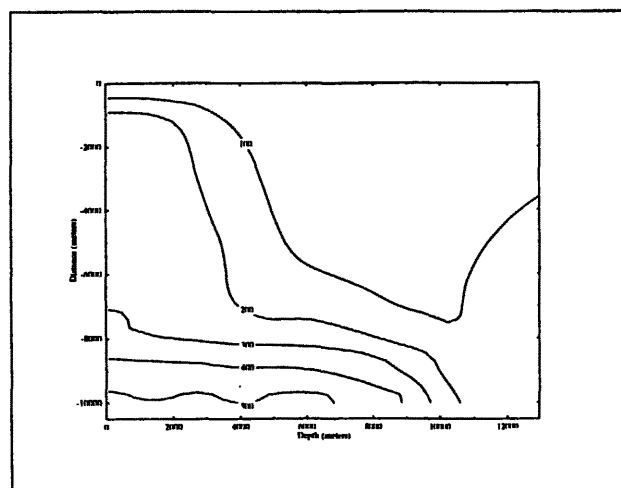
Figure 11. Temperature at 600,000 years.

in permeability as a result of deposition or dissolution is calculated using the methods derived by Weir and White (1996).

In Figure 8 we present contours of the log of the permeability reduction factor after simulation of the reservoir for 100,000 years. At the very base of the model, permeability is increased by a factor of ten as a significant amount of rock is dissolved in the hot (500° C) fluid at the base of the model. Above this is a region of reduced permeability caused by precipitation of silica as the fluid rises and cools. This layer has a permeability reduction factor of about .1, and covers the source from a depth of about 8km to 9.5 km. Above this at about 8km is a narrow layer with a permeability reduction factor of about .01. This coincides with the region containing water near the critical point and thus a minimum in silica solubility. It is also the area in which boiling began during the evolution of the field. Temperature profiles at this time are shown in Figure 9.

Figure 10 shows contours of permeability reduction at 600,000 years. The pattern is similar to those at earlier times, with a further reduction in permeability to about .01 of the original value below a depth of 8 km. By this stage the reservoir is all single-phase liquid so the rapid change in permeability around 8km depth must be caused by the minimum in silica solubility around the critical point. In the reservoir above 8km there is a zone of deposition from the origin out to about two kilometers and between 7.5 and 4.5 km depth. At earlier times, this would have been in the center of the rising plume of hot fluid. As the field evolves, this area of reduced permeability changes the flow patterns in the reservoir, forcing the plume out towards the outer edge of the model. From the temperature contours shown in Figure 11 it appears that energy transfer below 8km is largely conductive, with a convective cell above 8km.

Conclusions

It is possible by including some chemical species in geothermal reservoir models to estimate the variation of chemical conditions throughout the reservoir. We have illustrated this with a simple model of the Rotokawa reservoir and modelled the formation of acid sulphate and neutral pH bicarbonate waters near the surface.

The work on silica transport presented here suggests that for super-critical reservoirs permeability may be poor in areas of permeability near the critical point. This lack of permeability is caused by a minimum of silica solubility at these temperatures and pressures. Below this area of low permeability there may be an area on enhanced permeability although the nature of this permeability and its duration remain an open question as plastic deformation of the rocks my destroy the permeability.

In our modelling groundwater circulates to the base of the model for only a short time (<50,000 years) and at later times energy transport below 8km depth is largely conductive with a convection cell above this.

References

Bear, J., Nitao, J.J., (1995) On Equilibrium and Primary Variables in Transport in Porous Media, TIPM., 18 151-184, 1995.

Bird, G., Boon, J., Stone, T. 1986. Silica transport during steam injection into oil sands. 1. Dissolution and precipitation kinetics of quartz: new results and review of existing data. Chemical Geology, Vol.54: 69-80.

Dove, P.M. 1994. The dissolution kinetics of quartz in sodium chloride solutions at 25° to 300°C. American Journal of Science, Vol.294: 665-712.

Dove, P.M., Rimstidt, J.D. 1994. Silica-water interactions. Reviews in Mineralogy: Silica physical behaviour, Geochem & Materials Applications. Ed P J Henney, C T Prewitt & G U Gibbs.

Eugster, H.P. 1981. Metamorphic solutions and reactions. In Chemistry and geochemistry of solutions at high temperatures and pressures. Physics and Chemistry of the Earth Volumes 13 & 14. (eds. D T Rickard, F E Wickman): 461-507.

Fournier, R.O. 1983a. Self-sealing and brecciation resulting from quartz deposition within hydrothermal systems. Proceedings Fourth International Symposium on Water-Rock Interaction, Misasa, Japan: 137-140.

Fournier, R.O. 1985. The behaviour of silica in hydrothermal solutions. In Geology and Geochemistry of Epithermal Systems. Reviews in Economic Geology, Vol. 2.(eds. B R Gerger & P M Bethke). 45-72.

Fournier, R.O., Potter, R.W. II, 1982b. An equation correlating the solubility of quartz in water from 25°C to 900°C at pressures up to 10 000 bars. Geochimica et Cosmochimica, Vol.46: 1969-1973.

Friedly, J.C., Rubin, J., (1992) Solute Transport with Multiple Equilibrium-Controlled or Kinetically Controlled Chemical Reactions, Water Resour. Res., 28, 1935-1953, 1992.

Kissling W.M., Brown, K.L., O'Sullivan, M.J., White, S.P., Bullivant, D.P. (1996) Modelling Chloride and CO_2 Chemistry in the Wairakei Geothermal Reservoir, Geothermics, 25 285-306 (1996)

Kissling W.M. (1997) The Large Scale Structure of the Geothermal Fields in the Taupo Volcanic Zone, New Zealand , Submitted to Journal of Volcanology and Geothermal Research (1997)

Lasaga, A.C. 1984. Chemical kinetics of water-rock interactions. Journal of Geophysical Research, Vol.89: 1009-1025.

Lichtner, P.C. (1992) Time-Space Continuum Description of Fluid/Rock Interaction in Permeable Media. Water Resour. Res., 28 3135-3155 1992.

Manning, C.E. 1994. The solubility of quartz in H_2O in the lower crust and upper mantle. Geochimica et Cosmochimica Acta, Vol.58: 4831-4839.

Murphy, W M, Helgeson, H C 1989. Thermodynamic and kinetic constraints on reaction rates among minerals and aqueous solutions. IV. Retrieval of rate constants and activation parameters for the hydrolysis of Pyroxene, Wollastonite, Olivine, Andalusite, Quartz, and Nepheline. American Journal of Science, Vol. 289: 17-101.

Pruess, K. (1991), TOUGH2 - A General-purpose numerical simulator for multiphase fluid and heat flow., Report LBL-29400, Lawrence Berkeley Laboratory. 1991.

Reed, M.H., Spycher, N.F. (1992), SOLTHERM: Data Base of Equilibrium Constants for Aqueous-Mineral-Gas Equilibria Report, Department of Geological Sciences, University of Oregon, Eugene, Oregon 97403} 1992.

Rimstidt, J.D., Barnes, H.L. 1980. The kinetics of silica-water reactions. Geochimica et Cosmochimica Acta, Vol.44: 1683-1699.

Steefel, C.I., Lasaga, A.C. 1994. A coupled model for transport of multiple chemical species and kinetic precipitation/dissolution reactions with application to reactive flow in single phase hydrothermal systems. American Journal of Science, Vol.294: 529-592.

Tester, J.W., Worley, G., Robinson, B.A., Grigsby, C.O., Feerer, J.L. 1994. Correlating quartz dissolution kinetics in pure water from 25 to 625°C. Geochimica et Cosmochimica Acta, Vol.58: 2407-2420.

Weir, G.J., White, S.P (1996) Surface Deposition from Fluid Flow in a Porous Medium TIPM 25: 79-96 (1996).

White, S.P. (1995) Multiphase nonisothermal transport of systems of reacting chemicals, Water Resour. Res., 31 1761-1772 (1995).

White, S.P. Kissling W.M. (1996) Proc. New Zealand Geothermal Workshop (1996)

Xie, Z., Walther, J.V. 1993. Wollastonite + Quartz solubility in supercritical NaCl aqueous solutions. American Journal of Science, Vol.293: 235-255.